An Investigation of the Efficacy of Using Strain Gauge Arrays to Measure Axial and Shear Femur Forces in Post-Mortem Human Subjects

Devon L. Albert, Warren N. Hardy, Andrew R. Kemper

Abstract Lower extremity injuries are prevalent in motor vehicle collisions. Therefore, it is necessary to accurately quantify lower extremity kinetics in order to evaluate strategies for mitigating these injuries. Current methods for quantifying lower extremity loads in post-mortem human subjects (PMHS) have limitations that could affect the accuracy of the measured loads. Hence, the purpose of this study is to evaluate the efficacy of using strain gauge arrays (SGAs) to quantify axial and anterior-posterior shear femur forces in PMHS during full-scale frontal sled tests. Six PMHS were instrumented with SGAs to measure bilateral axial and shear femur forces before undergoing frontal sled tests. Several calibration procedures were performed to convert the SGA outputs (mV) to forces. The resulting forces were compared to knee bolster reaction forces and femur forces from matched sled tests performed using anthropomorphic test devices. Overall, the PMHS SGAs measured reasonable axial forces during the sled tests, but more work is necessary to validate the shear forces. Given the degree of crosstalk observed during the calibration procedure, future studies should use axial, anterior-posterior shear, and medial-lateral shear SGAs together to facilitate full crosstalk compensation. Furthermore, precise post-test calibrations capable of evaluating crosstalk should be performed on long bones instrumented with SGAs.

Keywords *Anthropometric test devices,* Crosstalk, Frontal impact, Lower extremity kinetics, Motor vehicle collision.

I. INTRODUCTION

Injuries to the lower extremity are still common in motor vehicle collisions (MVCs). It is estimated that the floor and/or foot pedals contribute to 93% of lower leg injuries, while contact with the knee bolster or instrument panel contributes to 87% of upper leg injuries. Loading of the lower extremity via the floor and toe pan intrusion has been demonstrated to increase the likelihood of lower extremity injuries [1].

In order to mitigate the risk and/or severity of these injuries, it is necessary to measure post-mortem human subject (PMHS) lower extremity loads. Lower extremity forces can be used to develop new injury risk prediction methods or to evaluate current methods. Additionally, PMHS lower extremity kinetics are needed to validate the responses of new anthropomorphic test devices (ATDs), such as the Test device for Human Occupant Restraint (THOR). Finally, accurate measurement of lower extremity loads is necessary to evaluate new safety restraint systems, such as knee bolster airbags, which are intended to decrease the peak magnitude of the load that would normally be transmitted to the lower extremity via contact with the knee bolster.

Although several studies have evaluated lower extremity loading in PMHS, there are several limitations with the methods that have been used to quantify it. One method is to implant a load cell into a long bone [2-7], but there are several limitations with this approach. First, the metal load cell and potting compound used to implant the load cell are likely different in both stiffness and mass than the section of bone being replaced. Therefore, implanting the load cell can alter the stiffness of the bone as a whole, which could then bias the load measurement. Furthermore, the altered mass and inertial properties could affect any kinematics and kinetics that may be of interest during an experiment. Finally, implanting a load cell can cause stress concentrations at the implantation site. This could alter the fracture timing and fracture pattern of the bone, biasing any injury assessments [3]. Another less invasive method for quantifying axial loads and bending moments in the lower extremity involves placing several strain gauges on the bone to measure the local strain field [8]. Then, three-

D. L. Albert (phone: +1-540-231-1890, e-mail: dla16@vt.edu) is a Postdoctoral Associate at Virginia Tech in Blacksburg, VA, USA. D. L. Albert, W. N. Hardy (Associate Professor) and A. R. Kemper (Assistant Professor) are all affiliated with the Center for Injury Biomechanics (CIB) at Virginia Tech.

point bending tests and beam theory are used to calibrate the strain field to the axial force and bending moment experienced by the bone. The limitations with this approach are due to the assumptions associated with beam theory. Namely, that there is no curvature to the femur and that the modulus of the bone is constant regardless of strain rate.

A recent study developed a preliminary method for measuring lower extremity loads during underbody blast using strain gauge arrays (SGAs) on the femur and tibia [9]. This method is minimally invasive and does not rely on beam theory assumptions. However, the approach has not yet been applied or validated under an MVC loading scenario. The purpose of this study was to evaluate the efficacy of using strain gauge arrays (SGAs) to quantify axial and shear femur forces in PMHS during full-scale frontal sled tests.

II. METHODS

Full-scale sled tests using 50th percentile male PMHS, the 50th percentile male Hybrid III (HIII), and the 50th percentile male THOR-M were performed as part of a larger study. The full methodology for the study is presented in [10]. Briefly, the sled tests were designed to replicate the 2005 and 2012 Toyota Camry New Car Assessment Program (NCAP) tests (ΔV = 56 km/h, peak acceleration = 470 m/s^2). A custom buck, designed using the interior measurements of a 2013 Toyota Camry, was used for each test (Fig. 1). The buck incorporated Toyota Camry vehicle components, including a seat, seatbelt system with pretensioner and load limiter, steering column, steering wheel, and steering wheel airbag module. Three restraint conditions were evaluated for each surrogate, but only two conditions were included in the current study. The ATDs each underwent two tests with a knee bolster and steering wheel airbag (KB/SWAB) and two tests with a knee bolster airbag and steering wheel airbag (KBAB/SWAB). Three PMHS were tested under the KB/SWAB condition, while an additional three PMHS were tested under the KBAB/SWAB condition. All PMHS were approximately 50th percentile males, and each PMHS underwent only one sled test. Subject demographics and anthropometry data have been previously reported [10][11]. Rigid polyurethane foams with strength ratings of 65 and 19 psi were used to simulate the KB and KBAB, respectively [12]. The left and right KB and KBAB foams were distinct, and were mounted to supports on the left and right side of the steering column. Each support was equipped with a six-axis load cell (Model 2513, Robert A. Denton, Inc., Rochester Hills, MI, USA) to quantify reaction loads at the bolster. To measure surrogate femur loads, the HIII and THOR-M were instrumented with six-axis loads cells in the left and right femurs (HIII: Model 1914A, Robert A. Denton, Inc., Rochester Hills, MI, USA; THOR-M: Model W5071010S1, Humanetics Innovative Solutions, Farmington Hills, MI, USA). The PMHS were instrumented with two sets of SGAs at approximately the mid-diaphysis of the left and right femurs for a total of 12 femurs instrumented with SGAs. One set of SGAs was designed to quantify the axial load (Fz) on the femur. The other set was designed to quantify the anterior-posterior (AP) shear force (Fx) on the femur. The design and instrumentation methodology of the SGAs are presented in the following section.

During the sled tests, data were collected from the reaction load cells, ATD load cells and SGAs at 20 kHz. The bolster reaction loads and moments were filtered at SAE channel frequency class (CFC) 60 [13]. The ATD femur forces and moments and the PMHS SGA outputs were filtered at CFC 600. The only exception was the HIII right femur axial force, which was filtered at CFC 180 to minimise excessive noise spikes.

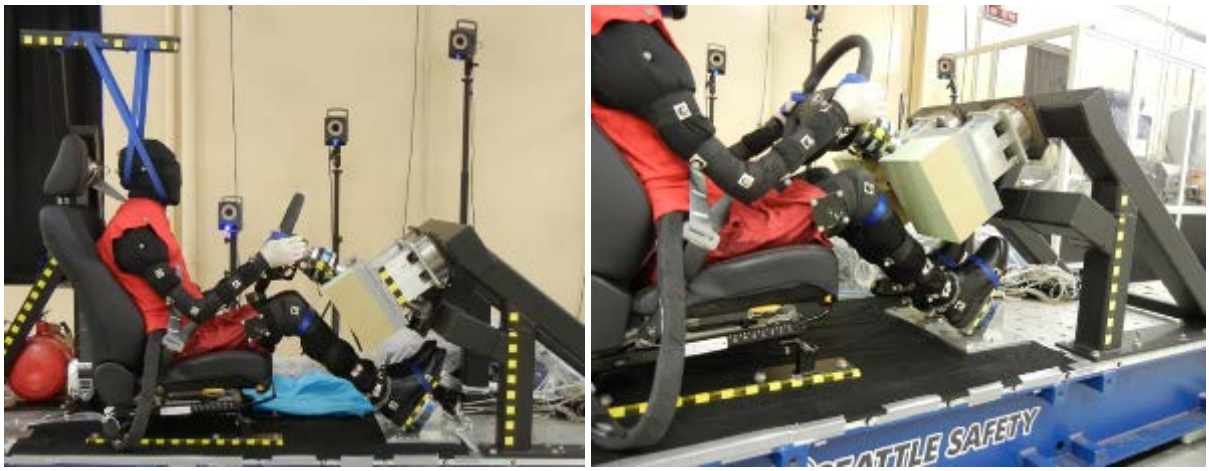

Fig. 1. Example PMHS sled test setup for KB/SWAB condition.

SGA Instrumentation

The axial and shear SGAs each consisted of four strain gauges arranged in a bridge configuration (Fig. 2 and Fig. 3). For the axial SGAs, four two-axis (CEA-06-125UT-350, Vishay Micro-Measurements, Raleigh, NC, USA) strain gauges were arranged at approximately equidistant locations around the circumference of each femur. To ensure the strain gauges are in the optimal positions, the horizontal centrelines of each gauge were aligned with each other and the vertical centrelines were aligned with the long axis of the femur. The configuration of the strain gauges on the femur and within the bridge circuit allowed the voltage output of the bridge circuit to be linearly related to the axial force experienced by the femur. For the shear SGAs, two pairs of single axis strain gauges (CEA-06-250UW-350, Vishay Micro-Measurements, Raleigh, NC, USA) were positioned on the anterior and posterior aspects of the femur. The two gauges on anterior surface were positioned several centimetres apart with their vertical centrelines aligned to the long axis of the femur. The remaining two gauges were positioned on the posterior surface of the femur, directly behind the gauges on the anterior surface. This configuration allowed the voltage output of the bridge circuit to be linearly related to the AP shear force experienced by the femur, independent of the point of application.

A detailed procedure was followed to apply the strain gauges to the femurs. The soft tissue and periosteum were removed from the mid-diaphysis of the femur, and the exposed bone was cleaned with isopropyl alcohol and dried with acetone. A catalyst (M-Bond 200 Catalyst, Vishay Micro-Measurements, Raleigh, NC, USA) was applied to the bone and the back of each strain gauge before the gauge was adhered to the bone. The adhesive (M-Bond 200 Adhesive, Vishay Micro-Measurements, Raleigh, NC, USA) was first applied to the gauge, then the gauge was positioned on the bone and held in place with pressure for several minutes. A protective coating (M-Coat-D Adhesive, Vishay Micro-Measurements, Raleigh, NC, USA) was applied to the top of the gauge and the bone immediately surrounding the gauge in order to protect the gauge from moisture.

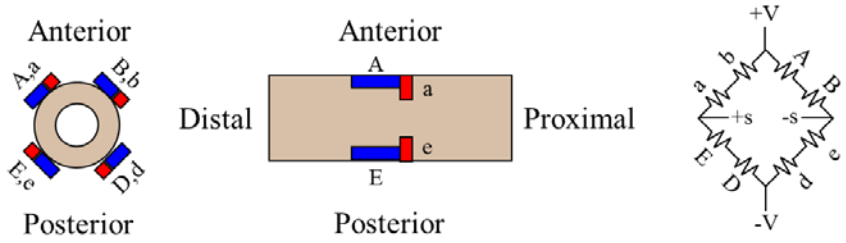

Fig. 2. Axial SGA configuration and bridge circuit.

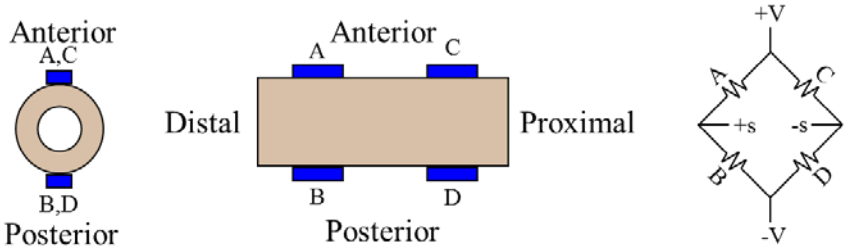

Fig. 3. AP shear SGA configuration and bridge circuit.

Pre-Test Calibrations

In order to convert the outputs (mV) of the axial and shear SGAs to forces for each femur, a pre-test calibration procedure was performed before each sled test. The calibration procedure involved imposing forces upon the lower extremity of the prone PMHS while simultaneously recording output from the SGAs and a hand-held uniaxial load cell (Model 1516, Robert A. Denton, Inc., Rochester Hills, MI, USA). To calibrate the axial SGAs, the hip and knee were flexed to approximately 90 degree angles, such that the femur was perpendicular to the ground and the shank was parallel to the ground. By approximately aligning the centre of the load cell with the long axis of the femur and pressing the load cell against the skin superficial to the knee cap, an axial force was transmitted through the load cell to the femur. To calibrate the shear SGAs, the hip or proximal end of the femur was placed

on a rigid support so that the knee was elevated and unsupported. While keeping the hip stable, the load cell was placed against the skin superficial to the anterior surface of the distal femur and the leg was pushed downward, creating an AP shear force. All data from the SGAs and load cell were collected at 250 Hz.

In order to generate a calibration factor to convert the SGA output to the corresponding force, the loading phase of the SGA output and load cell output during the pre-test calibration were plotted and fit with a linear trend line (Fig. 4). The slope of the trend line was used as a calibration factor to convert the SGA output during the sled tests to axial force and shear force (Fig. 5). During all pre-test calibrations, both the axial and shear SGA outputs were recorded in order to account for crosstalk between the axial and shear SGAs. However, a consistent relationship was not always observed between the on-axis load and the off-axis SGA; therefore, crosstalk could not be evaluated or applied to the sled test data.

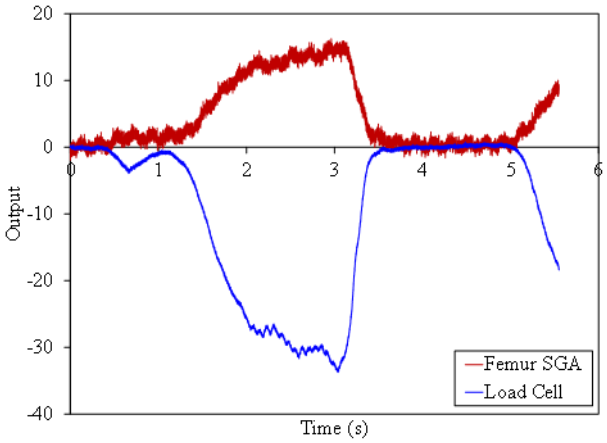

Fig. 4. Example axial pre-test calibration output.

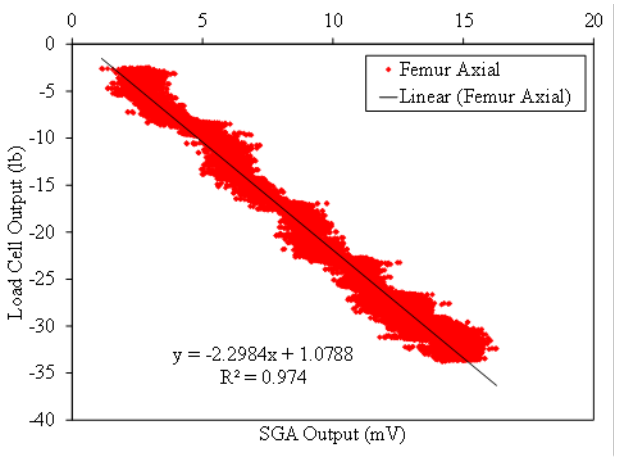

Fig. 5. Example trend line fit to load cell and SGA outputs.

Post-Test Calibrations

In order to obtain more precise calibration factors and to evaluate the degree of crosstalk between SGAs, post-test calibrations were performed after the sled tests. The post-test calibration procedure involved exposing the femurs to pure axial and shear loads after a precise potting process. After each sled test, the femurs of the tested PMHS were dissected and examined for injuries. No injuries were observed for any of the femurs. The femurs were then frozen until all sled tests had been completed. Before the potting process, a given femur was thawed and all tissue was removed from the diaphysis. The femur was then cut to a specific length of diaphysis encompassing the SGAs, which was mounted into a custom potting jig (Fig. 6 and Fig. 7) with the distal end of the diaphysis centred in a potting cup. Laser levels located 90 degrees apart were used to ensure the long axis of the femur was aligned with the centre of the potting cup by moving the femur until the laser lines were centred on the anterior and left aspects of the femur. The distal end of the diaphysis was then potted using EasyFlo 60 Liquid Plastic (Polytek Development Corp., Easton, PA, USA). After the potting compound finished curing the femur was rotated 180 degrees, using a custom jig (Fig. 8), so that the proximal end of the diaphysis was centred in a potting cup that was concentric with the distal potting cup. Additionally, the jig ensured that the top and bottom surfaces of the distal and proximal potting cups were perfectly parallel. The proximal diaphysis was then potted using the same method as the distal diaphysis. After the potting process, the femurs were refrozen until all femurs had been potted and the axial and shear testing fixtures had been setup. While being stored, the femurs were wrapped in saline-soaked paper towels and sealed in a plastic bag. Before the post-test calibrations were performed, all femurs were allowed to thaw at room temperature for at least 36 hours.

The shear force calibration test was performed by cantilevering a five-axis load cell (Model 1968, Robert A. Denton, Inc., Rochester Hills, MI, USA) in series with the potted femur and suspending a series of weights from the distal potting cup (Fig. 9). A Kevlar string was used to attach a carabiner to the distal potting cup. Five increments of 2.27 kg (5 lbs) weights were then attached to the carabiner via Kevlar string. This resulted in five distinct loading steps that together totaled approximately 11.34 kg (25 lbs) at the end of the test. To quantify the output of the axial and AP shear SGAs while an AP shear force was applied, the femur was oriented with the anterior aspect upwards so that a force was applied in the posterior direction at the distal diaphysis when the weights were applied. Additionally, the outputs of the axial and AP shear SGAs were quantified while the femur

experienced a medial-lateral (ML) shear force. This was accomplished by rotating the femur 90 degrees about the long axis, so that the left aspect of the femur faced upward, and applying a force to the right at the distal diaphysis. All SGA and load cell data were collected at 250 Hz during the shear force calibration tests.

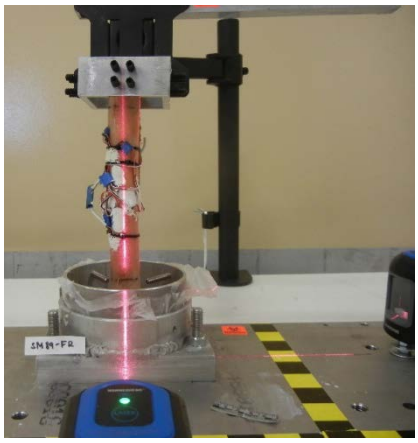

Fig. 6. Custom jig for aligning and potting the distal femur (anterior view).

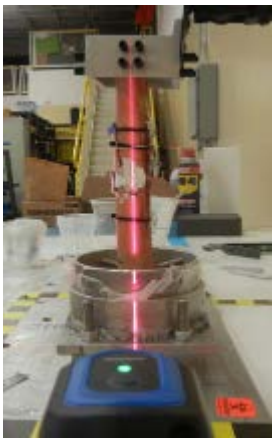

Fig. 7. Custom jig for aligning and potting the distal femur (left view)

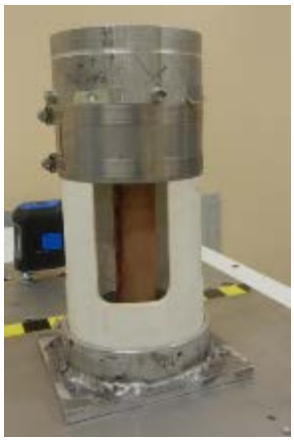

Fig. 8. Custom jig for potting the proximal femur (right view).

The axial force calibration test was performed using a custom test fixture designed to translate a platform vertically with minimal rotation (Fig. 10) [14]. The platform was raised and lowered via winch and guided by eight linear bearings on four linear rails. A five-axis load cell (Model 1968, Robert A. Denton, Inc., Rochester Hills, MI, USA) was placed in series with the potted femur below the centre of the platform. Additionally, a ball bearing was placed between the femur and the platform so that lowering the platform onto the bearing transmitted a force through the long axis of the femur and load cell with negligible induced moments. During an axial force calibration test, the platform was lowered onto the ball bearing, placing approximately 16 kg (35 lbs) of mass onto the femur. Subsequently, six 4.5 kg (10 lbs) weights were added incrementally to the centre of the top face of the platform, resulting in a total of 43 kg (95 lbs) at the end of the test. The axial and shear SGA outputs and load cell data were collected at 250 Hz during the axial calibration tests.

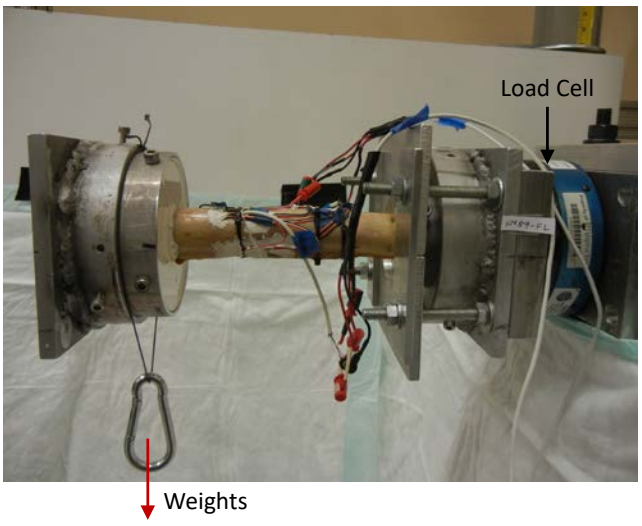

Fig. 9. Shear post-test calibration setup.

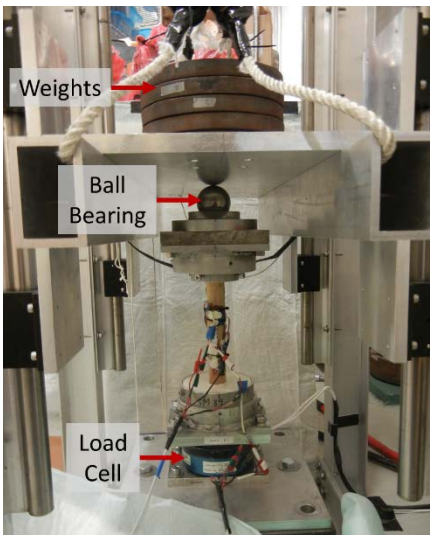

Fig. 10. Axial post-test calibration setup.

Calibration factors and crosstalk matrices were generated for each femur from the post-test calibrations using the following procedure. First, loading steps generated by adding weights incrementally during the test were averaged over time for each signal to obtain a single value for each step, representing the load cell or SGA output during a particular weight increment. For example, the shear force calibration tests consisted of five weight increments, so six points (including zero) were generated for each SGA and load cell axis. The averaged points for each SGA were then plotted against the averaged points from the load cell axis in the direction of loading (Fig. 11

and Fig. 12). Then, the resulting relationship was fit with a linear trend line (Fig. 13 and Fig. 14). The slope of the trend line either was used to generate a direct calibration factor between the load cell and SGA (no crosstalk) or was used as a component to generate a crosstalk matrix. A 2 by 2 (axial and AP shear) crosstalk matrix was calculated using the slopes from the following relationships: load cell axial force vs SGA axial output (k_1), load cell AP shear force vs SGA axial output (k_2), load cell axial force vs SGA AP shear output (k_3), and load cell AP shear force vs SGA axial (k_4). The slopes were then arranged into a matrix according to Equation 1:

$$\begin{bmatrix} SGA_Z \\ SGA_X \end{bmatrix} = \begin{bmatrix} k_1 & k_2 \\ k_3 & k_4 \end{bmatrix} \begin{bmatrix} LC_Z \\ LC_X \end{bmatrix}, \quad (1)$$

where SGA_Z is the axial SGA output (mV), SGA_X is the AP shear SGA output (mV), LC_Z is the axial load cell force (N), LC_X is the AP shear load cell force (N), and k_1, k_2, k_3 and k_4 are the slopes from the relationships described above, each with units (mV/N). Calculating the inverse of the 2 by 2 slopes matrix generated the crosstalk matrix. Applying the crosstalk matrix to the SGA outputs during the sled tests allowed the calibration and crosstalk to be applied at the same time, generating crosstalk compensated axial and shear forces.

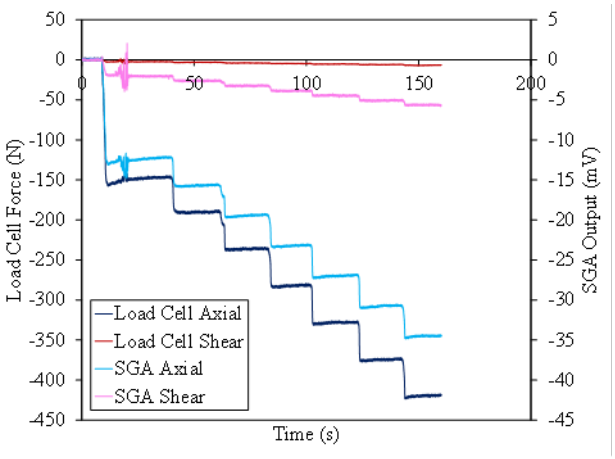

Fig. 11. Example axial post-test calibration load cell and SGA outputs.

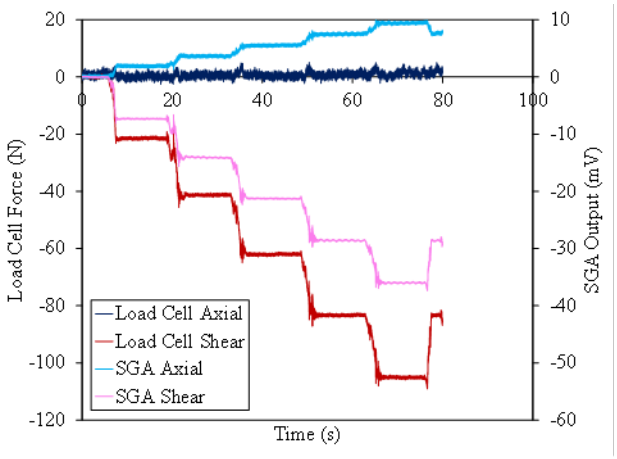

Fig. 12. Example shear post-test calibration load cell and SGA outputs.

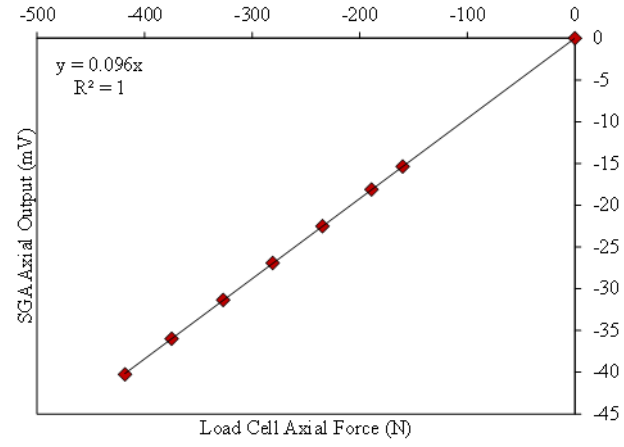

Fig. 13. Example trend line fit to axial load cell and axial SGA outputs.

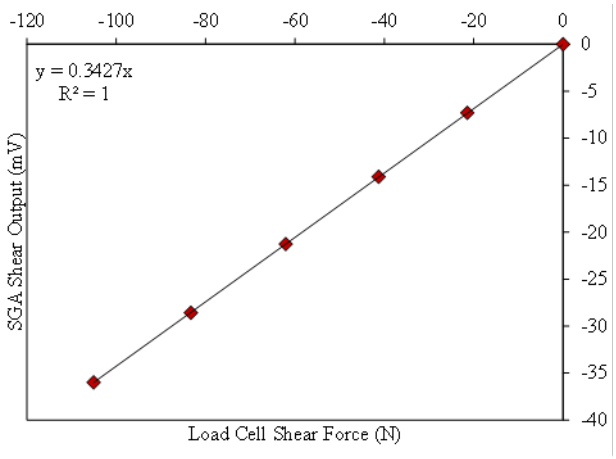

Fig. 14. Example trend line fit to shear load cell and shear SGA outputs.

Data Analysis

Several analyses were undertaken to evaluate the different SGA calibration methods. The effect of crosstalk on each of the SGA forces was evaluated by calculating the percent difference between the peak sled test force generated using the crosstalk matrix and the peak sled test force generated by directly applying the calibration factor without accounting for crosstalk. Additionally, differences between the pre-test and post-test calibrations were evaluated by calculating the percent difference between the peak sled test force generated using the pre-test calibration and the peak sled test force generated using the post-test calibration for each SGA axis and femur.

Crosstalk due to ML loading could not be included in the crosstalk matrix because the femurs were not instrumented with SGAs in the ML configuration. Therefore, the sensitivities of the axial and AP shear SGAs to ML loading were evaluated by comparing the slope of the relationship between the SGA outputs and ML load to the slope of the relationship between SGA outputs to same-axis loading (e.g. SGA axial output to load axial force during an axial calibration test). A higher slope from an ML test would indicate that an SGA is more sensitive to ML loading than same-axis loading. Conversely, a higher slope during a same-axis test would indicate an SGA is more sensitive to same-axis loading than ML loading.

In an attempt to evaluate the accuracy of the forces quantified using the SGAs, the SGA forces were compared to the reaction knee bolster forces. Even though it has been shown that the stiffness of the PMHS, HIII and THOR femurs are different [15], Newton's third law implies that the ratio between the femur force and bolster reaction force should be comparable between the PMHS and ATDs. Therefore, the accuracy of the quantified PMHS femur forces was evaluated by calculating the average ratio between the femur and bolster forces for each surrogate and assessing whether the ratio for the PMHS was similar to the ratios for the ATDs. A similar ratio would indicate that the SGA forces are reasonable. This analysis was first performed using the resultant (Fx and Fz) femur and bolster forces because the orientation of the bolster reaction load cell relative to the femur changes throughout the duration of the test, so the components cannot be directly compared without additional calculations. The ratios were calculated at two time points: the time of peak femur resultant force and the time of peak bolster resultant force. In order to evaluate the accuracy of the individual SGAs (i.e. axial and AP shear), the axial and shear bolster forces were adjusted to correspond to the orientation of the femur at the time of peak knee excursion. The femur orientation at peak knee excursion was used because this roughly corresponded with the time of peak resultant bolster force and peak axial femur force. The femur orientation for each surrogate at the time of peak knee excursion was calculated using high-speed video still frames. The ratios of the femur and adjusted bolster were then calculated in the directions corresponding to femur axial and AP shear forces. The axial force ratios were calculated at the times of peak femur axial force and peak bolster resultant force. The shear force ratios were calculated at the times of peak femur shear force and peak bolster resultant force.

III. RESULTS

Both axial and shear forces were calculated for successfully nine of the 12 femurs tested. Two femurs in the KB/SWAB condition had unreasonably large axial forces, as calculated from the SGAs, but had normal shear forces and normal post-test calibrations. Therefore, it is hypothesised that the axial SGAs malfunctioned due to moisture or direct pressure applied to the gauges. A shear gauge on a femur in the KBAB/SWAB condition delaminated at an unknown time after application. Initial post-test calibrations resulted in unreasonably low shear forces. The gauge was identified and re-glued into approximately the same position as before. However, calibrations performed after this modification resulted in unreasonably high shear forces, which suggests that the gauge likely delaminated before the sled test.

Crosstalk was only applied to femurs where both the axial and shear forces were calculated successfully. Therefore, nine femurs had calibrations applied via post-test crosstalk calibration, post-test direct calibration (no crosstalk), and pre-test calibration. The post-test calibration factors without crosstalk were directly applied to generate shear forces for two femurs and axial force for one femur. Pre-test calibrations were also applied to these femurs. Compared to the sled test forces generated using the direct post-test calibration, applying a crosstalk calibration decreased the peak sled test axial force for six out of nine femurs and decreased the peak sled test shear force for three out of nine femurs. The average absolute percent difference between the crosstalk and no crosstalk peak axial forces was 9% ± 5%. The minimum and maximum percent differences were 0.3% and 15%, respectively. For the shear forces, the average percent difference was 20% ± 19%. The minimum and maximum percent difference for the shear forces were 0.2% and 64%, respectively.

Greater differences were observed between the pre-test and post-test calibrations for the shear force than for the axial force. For these comparisons, the crosstalk post-test calibration was applied to sled test data for the nine femurs where both the axial and shear SGAs functioned during the sled tests. The direct post-test calibration was applied to the remaining SGAs. When compared to the pre-test calibrations, the post-test calibrations resulted in higher peak sled test forces for all 10 of the axial SGAs and three of the 11 shear SGAs. The average absolute percent difference between the pre- and post-test calibrations were 25% ± 18% and 39% ± 27% for the axial and shear forces, respectively. For the axial forces, the minimum and maximum percent differences were

0.2% and 60%, respectively. For the shear forces, the minimum and maximum percent differences were 9% and 103%, respectively.

The axial SGAs were more sensitive to ML loading than the AP shear gauges. However, a consistent trend between the axial SGA and ML loading was not observed for one femur in the KBAB/SWAB condition, so it was not included in the analysis. Six out of 11 of the axial SGAs had a greater sensitivity to ML loading than axial loading. An additional three axial SGAs were at least half as sensitive to ML loading as they were to AP loading, i.e. the slope of the trend between axial SGA output and applied ML load was at least 50% of the slope between axial SGA output and applied axial load. On average, the axial SGAs were 1.19 times more sensitive to ML loading than axial loading. Conversely, only two of the 12 shear SGAs had a greater sensitivity to ML loading than AP loading. An additional four shear SGAs were at least half as sensitive to ML loading as they were to AP loading. Additionally, the AP shear SGAs were 1.72 times more sensitive to AP shear loading than ML shear loading, on average.

To evaluate the accuracy of the SGA forces, the ratio of the femur forces and bolster forces were compared between surrogates. For the ratios of the resultant femur and bolster forces (Table I, Table II, Fig. 15 and Fig. 16), the PMHS ratio was similar to the ATD ratios for the KB/SWAB condition, but the PMHS ratio was higher than the ATD ratios for the KBAB/SWAB condition. This was due to one particular PMHS femur that had a much higher ratio than all of the other PMHS femurs. It should be noted that there was a much larger difference in the peak femur and bolster times for this particular femur compared to the others, indicating that there was a phasing issue with this comparison. Excluding this test from the calculated ratios resulted in PMHS ratios that were similar to the ATDs for both conditions and time points. A similar trend was seen for the axial force ratios (Table III and Table IV), where the PMHS and ATD ratios were reasonably similar after the one KBAB/SWAB test was excluded. However, clear discrepancies existed between the different surrogates for the shear force ratios (Table V and Table VI). The HIII had extremely high ratios compared to the other two surrogates, and the PMHS had the lowest ratios. It should be noted that the phasing issue with the KBAB PMHS femur in the axial and resultant ratios was not an outlier in the shear ratios, indicating that the phasing issue was due to the axial force.

TABLE I
RESULTANT FORCE RATIOS AT PEAK BOLSTER FORCE

Condition	HIII	THOR	PMHS
KB/SWAB	0.49	0.48	0.46
KBAB/SWAB	0.61	0.53	0.80 (0.72)
All	0.55	0.51	0.65 (0.59)

Values in () excluded one test

TABLE II
RESULTANT FORCE RATIOS AT PEAK FEMUR FORCE

Condition	HIII	THOR	PMHS
KB/SWAB	0.53	0.61	0.54
KBAB/SWAB	0.68	0.87	0.98 (0.80)
All	0.60	0.74	5.98 (0.69)

Values in () excluded one test

TABLE III
AXIAL FORCE RATIOS AT PEAK BOLSTER FORCE

Condition	HIII	THOR	PMHS
KB/SWAB	0.48	0.49	0.46
KBAB/SWAB	0.60	0.52	0.80 (0.73)
All	0.54	0.51	0.66 (0.61)

Values in () excluded one test

TABLE IV
AXIAL FORCE RATIOS AT PEAK FEMUR FORCE

Condition	HIII	THOR	PMHS
KB/SWAB	0.52	0.63	0.54
KBAB/SWAB	0.66	0.84	1.00 (0.85)
All	0.59	0.74	0.81 (0.71)

Values in () excluded one test

TABLE V
SHEAR FORCE RATIOS AT PEAK BOLSTER FORCE

Condition	HIII	THOR	PMHS
KB/SWAB	0.74	0.23	0.46
KBAB/SWAB	17.0	4.31	0.54
All	8.86	2.27	0.50

TABLE VI
SHEAR FORCE RATIOS AT PEAK FEMUR FORCE

Condition	HIII	THOR	PMHS
KB/SWAB	2.77	1.25	0.58
KBAB/SWAB	12.8	2.91	1.70
All	7.79	2.08	1.09

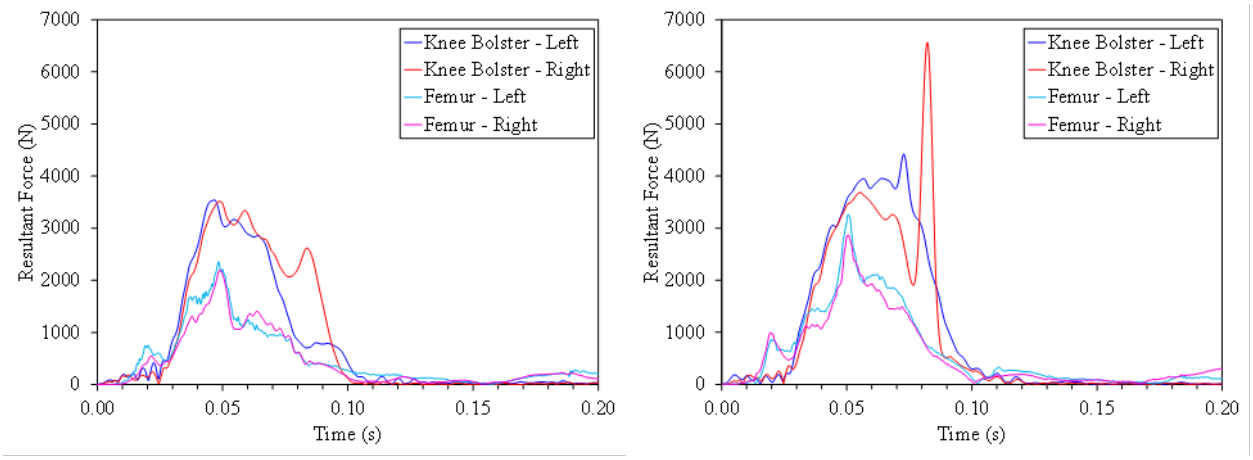

Fig. 15. Exemplar femur and bolster resultant forces for the KBAB/SWAB condition for the HIII (*left*) and THOR-M (*right*). (Note: the larger peaks at the end of the THOR-M bolster forces were due to the arms of the THOR-M hitting the bolster support structure. These peaks were excluded from the analysis.)

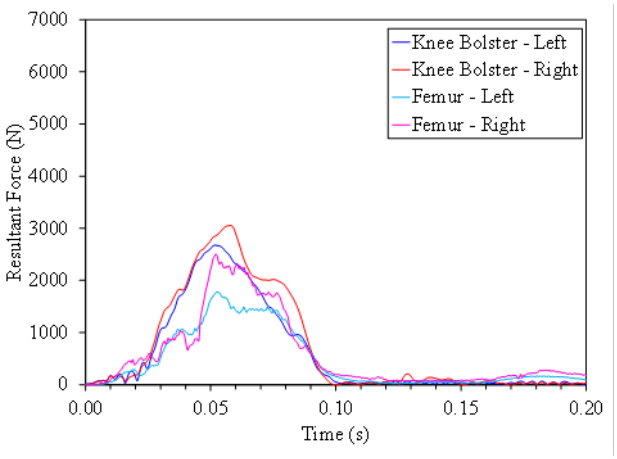

Fig. 16. Exemplar femur and bolster resultant forces for the KBAB/SWAB condition for the PMHS.

IV. DISCUSSION

The comparisons between the post-test and pre-test calibrations, as well as the comparisons between post-test calibrations with and without axial/AP shear crosstalk, indicate that the pre-test calibrations may not be adequate to serve as the only calibration procedure applied to the SGAs. A major limitation of the pre-test calibration procedure was that the SGAs could not be compensated for crosstalk between the axial and AP shear directions using that procedure. The effect of crosstalk on the axial SGAs was relatively low, with an average of 9% difference in peak force due to crosstalk and with a maximum of 15%. However, the average percent difference for the shear SGAs was 20%, with a maximum of 64%. For the shear SGAs in particular, the amount of crosstalk seems to be highly dependent on the femur and could greatly influence the calculated shear force. Therefore, accounting for crosstalk for the shear SGAs is necessary. Furthermore, the differences between the pre-test and post-test calibrations were non-trivial for both the axial and shear SGAs. The average percent difference between the pre- and post-test calibrations were 25% and 39% for the axial and shear forces, respectively. It should be noted that the post-test calibrations applied for this comparison included cross-talk. In the absence of the development of a more precise pre-test procedure that is capable of consistently measuring crosstalk, it is recommended that SGAs undergo a post-test calibration using the isolated femurs under various highly controlled loading conditions.

It is also recommended that SGAs are compensated for ML crosstalk. The axial SGAs, in particular, were highly sensitive to ML shear loading. Half of the axial SGAs were more sensitive to ML loading than axial loading. This may not have had a large impact on the axial forces in this study since the peak ML shear loads experienced by the ATD femurs were only 9% of the peak axial loads on average. The peak ML shear loads were 31% of the peak AP shear loads for the ATDs. However, the AP shear SGAs were less sensitive to ML shear loading compared to the axial gauges. Scenarios where there is more oblique loading on the femur could create large errors in the axial

forces calculated from the SGAs due to increased ML shear loading. Ideally, femurs should be instrumented with axial, AP shear and ML shear so that errors due to crosstalk can be minimised.

Based on the comparisons between the femur and bolster forces across surrogates, the axial forces calculated from the SGAs were reasonable; however, the shear forces seemed to be too low. Both the axial and resultant PMHS forces were reasonable compared to the ATD forces, indicating that the axial forces were the primary contribution to the resultant forces. The discrepancies between the PMHS and ATD AP shear forces may be a result of several factors. There were clearly large differences in phasing between the peak shear femur force and peak resultant force with the HIII, contributing to the very large femur to bolster ratios. It may be more appropriate to calculate the shear component of the bolster force that is aligned with the shear femur force throughout the duration of the test to find the true maximum shear bolster force. For the current study, it was assumed that the shear and axial forces would both peak at approximately the time of the peak resultant force. Additionally, the femur orientation at peak knee excursion was assumed to be similar to the orientation at the time of peak femur shear force. However, the phasing differences between the HIII peak bolster and femur forces indicate that the peak shear force may occur earlier during the test and at a different femur orientation. Ideally, the orientation of the femur throughout the test should be calculated and used to adjust the bolster force components into the correct orientations. However, that data are not currently available. In addition, the ML loading, which reached an average of 30% of the peak AP shear force in the ATDs, could be affecting the calculated AP forces through crosstalk.

Results from the preliminary designs of the SGAs used in the current study were presented in [9]. The authors noted that the axial SGAs in their study were more sensitive to AP shear loads than axial loads. In the current study, all but one axial SGA was more sensitive to AP shear loading than axial loads. However, the axial SGAs were less affected by crosstalk compensation than the AP shear SGAs. This is likely because the shear loads in the current study were much lower than the axial loads. Additionally, [9] noted that the shear gauges functioned better when the shear loading was predominantly through the knee as opposed to being distributed over the femur. This was not evaluated in the current study, but could also explain some of the discrepancies observed for the PMHS shear forces compared to the ATD shear forces. The KBAB and, to some extent, the KB foams can distribute some load over the anterior surface of the distal femur so loading may not be limited to the knee.

The method of validating the SGA outputs by comparing the ratio of internal femur forces and external bolster forces between PMHS and ATDs is limited by the assumption that force is transmitted from the knee to the femur load cell or SGAs similarly between PMHS and ATDs. A previous study showed that the HIII and THOR knee/femur complexes experience higher applied forces and demonstrate higher stiffnesses than PMHS knee/femur complexes under similar axial loading conditions [15]. However, the study did not report the ratio between the internal femur loads and the applied external loads at the knee. An older study that did compare this ratio between the HIII and PMHS at multiple loading rates found that the PMHS had an average ratio of 0.53, while the HIII had an average ratio of 0.68 [4]. The authors attributed the differences between the PMHS and HIII ratios to differences in effective accelerated mass between the PMHS and HIII, specifically any differences in mass distribution and load cell location between subject types. It has been shown that the thigh flesh in the HIII and THOR is more tightly coupled to the skeletal mass than in a PMHS, leading to differences in the effective mass between surrogate types throughout the duration of axial loading events [16]. However, [16] showed that the effective masses of the HIII, THOR, and 50th percentile male PMHS are similar at the time of peak applied force under femur loading rates comparable to those produced during NCAP tests. Since the tests in the current study were modeled after Toyota Camry NCAP tests, it may be reasonable to assume that the effective masses of the HIII, THOR-M, and PMHS used in the current study will be similar at the time of peak applied (bolster) force. Therefore, it could be assumed that the ratios of the internal femur forces and external bolster forces at the time of peak applied force would be similar across all surrogates. This is supported by the finding in [4] that the PMHS and HIII had similar ratios despite possible differences in load cell locations and effective masses.

Several limitations to the study may have influenced the results. First, the repeated freezing between the sled tests and post-test calibrations may have affected results. Similarly, local drying of the surface of the bone may have occurred during the potting and post-test calibration procedures since the femurs had to be exposed for long periods of time. Efforts were made to mitigate bone drying by wrapping the femurs in saline-soaked paper towels when the femurs were stored or frozen. Additionally, the crosstalk results could have been induced if the femurs were not perfectly centred within the potting cups. However, extreme care was taken to centre the bones

in the potting cups and the post-test calibration fixtures as well as possible. Furthermore, the off-axis load cell channels showed minimal loading during the post-test calibration data collection. Another limitation was that it was sometimes difficult to keep the strain gauges dry enough to obtain clear responses. Improved instrumentation may be needed to prevent moisture from affecting the gauges. Finally, several assumptions were made with regard to the calibrations and polarity. Namely, the current study assumed that a calibration factor for a particular direction of loading would be the same if the loading was applied in the opposite direction. For example, the calibration factor that was determined by loading the femurs in compression was also applied when the femurs were in tension during the sled tests. By extension, it was also assumed that the crosstalk between two axes would be the same regardless of polarity and that the polarity of the crosstalk would switch with the polarity of the loading. For example, if a negative AP shear force induced a compressive force reading in the axial SGA, it was assumed that the same amount of positive AP shear force would induce the same degree of tensile force in the axial SGA output. The validity of these assumptions was not evaluated in this study.

V. CONCLUSIONS

The results of the current study indicate that SGAs show promise as a minimally invasive method for measuring femur loads in PMHS; however, they require more investigation and validation before widespread implementation. Although the axial SGAs produced reasonable axial forces during the frontal sled tests, the shear forces were lower than expected. This may be partially a result of the relatively high amount of crosstalk between the axial, AP shear and ML shear axes. It is therefore recommended that all three axes be instrumented with SGAs and precise post-test calibrations be performed on all axes so that the SGAs can be adequately compensated for crosstalk. Future work will evaluate the use of axial and shear SGAs in the tibia in conjunction with the femur.

VI. ACKNOWLEDGEMENTS

The authors would like to acknowledge the support of the Toyota Motor Company for funding the sled tests performed as part of this study. The authors would also like to acknowledge Stephanie M. Beeman for her contributions to the sled tests and the pre-test SGA calibrations and Marieke Van Haaren for her contribution to potting the femurs for the post-test calibration. Finally, the authors would like to thank the anatomical donors whose generous gifts made this research possible.

VII. REFERENCES

[1] Austin, R.A. Lower Extremitty Injuries and Intrusion in Frontal Crashes. 2012, NHTSA: Washington, DC.

[2] Cheng, R., Yang, K.-H., Levine, R.S., and King, A.I. Dynamic impact loading of the femur under passive restrained condition. 1984, SAE Technical Paper.

[3] Dean-El, I., *et al*. Implantation design guidelines for instrumenting the cadaveric lower extremity to transduce femur loads and tibial forces and moments. 2003, SAE Technical Paper.

[4] Donnelly, B.R. and Roberts, D.P. Comparison of cadaver and hybrid III dummy response to axial impacts of the femur. 1987, SAE Technical Paper.

[5] Funk, J.R., Rudd, R.W., Kerrigan, J.R., and Crandall, J.R. The effect of tibial curvature and fibular loading on the tibia index. *Traffic Injury Prevention*, 2004. **5**(2): pp. 164–72.

[6] Funk, J.R., *et al.* Methodology for measuring tibial and fibular loads in a cadaver. 2002, SAE Technical Paper.

[7] McKay, B.J. and Bir, C.A. Lower extremity injury criteria for evaluating military vehicle occupant injury in underbelly blast events. *Stapp Car Crash Journal*, 2009. **53**: pp. 229–49.

[8] Untaroiu, C., *et al.* Correlation of strain and loads measured in the long bones with observed kinematics of the lower limb during vehicle-pedestrian impacts. *Stapp Car Crash Journal*, 2007. **51**: pp. 433–66.

[9] Danelson, K.A., *et al.* Comparison of ATD to PMHS response in the under-body blast environment. *Stapp Car Crash Journal*, 2015. **59**: pp. 445–520.

[10] Albert, D.L., Beeman, S.M., and Kemper, A.R. Occupant kinematics of the Hybrid III, THOR-M, and postmortem human surrogates under various restraint conditions in full-scale frontal sled tests. *Traffic Injury Prevention*, 2018. **19**(sup1): pp. S50–S58.

[11] Albert, D.L., Beeman, S.M., and Kemper, A.R. Assessment of thoracic response and injury risk using the Hybrid III, THOR-M, and post-mortem human surrogates under various restraint conditions in full-scale frontal sled tests. *Stapp Car Crash Journal*, 2018. **62**: pp. 1–65.

[12] Albert, D.L., Beeman, S.M., McNally, C., and Kemper, A.R. Evaluation of Rigid Polyurethane Foam as a Surrogate Material for Knee Bolsters and Knee Bolster Airbags in Full Scale Frontal Sled Tests. Short Communications From AAAM's 60th Annual Scientific Conference. *Traffic Injury Prevention*, 2016. **17**(sup1): pp. 205–8.

[13] SAE. Instrumentation for Impact Test - Part 1 - Electronic Instrumentation. 2014, SAE International.

[14] Fievisohn, E.M., Sajja, V.S.S.S., VandeVord, P.J., and Hardy, W.N. Evaluation of impact-induced traumatic brain injury in the Göttingen Minipig using two input modes. *Traffic Injury Prevention*, 2014. **15**(sup1): pp. S81–S87.

[15] Rupp, J., Reed, M., Madura, N., and Schneider, L. Comparison of knee/femur force-deflection response of the thor, hybrid III and human cadaver to dynamic frontal impact knee loading. *Proceedings of the International Technical Conference on the Enhanced Safety of Vehicles*, 2003, Nagoya, Japan.

[16] Rupp, J.D., Reed, M.P., *et al*. Comparison of the inertial response of the THOR-NT, Hybrid III, and unembalmed cadaver to simulated knee-to-knee-bolster impacts. *Proceedings of the 19th International Technical Conference on the Enhanced Safety of Vehicles, Paper*, 2005, Washington, D.C., USA.